Electronic Supporting Information

Rare Co/Fe-MOFs exhibiting high catalytic activity in electrochemical aptasensor for ultrasensitive detection of ochratoxin A

Zhen Wang, Hua Yu, Jing Han*, Gang Xie*, Sanping Chen

Key Laboratory of Synthetic and Natural Functional Molecule Chemistry of Ministry of Education, College of Chemistry & Materials Science, Northwest University, Xi'an, Shaanxi 710127, P. R. China.

Corresponding author: Dr. Jing Han and Prof. Gang Xie

E-mail address: hanjing@nwu.edu.cn (J. Han), xiegang@nwu.edu.cn (G. Xie).

Fax: +86 029 81535026; Tel: +86 029 81535026.

Experimental section

Reagents and materials

Gold chloride ($HAuCl_4$), thionine (Thi), tris(2-carboxyethyl)phosphine hydrochloride (TCEP), ethylenediaminetetraacetic acid (EDTA) and hexanethiol (HT) were supplied by Sigma Chemical Co. (St. Louis, USA). Gold nanostar (AuNs) was obtained from XF NANO (Nanjing, China). Ochratoxin A (OTA), zearalenone (ZEN), aflatoxin B_1 (AFB_1), terephthalic acid (BDC), 2-aminoterephthalic acid (NH_2-BDC), acetic acid (HAc), sodium acetate (NaAc) and triethylamine (TEA) were purchased from Aladdin Chemicals Co. Ltd. *N,N*-dimethylformamide (DMF) and other chemical reagents are analytical reagent (A.R.) grade.

The buffers involved in this experiment were prepared as follows: Phosphate buffered solution (PBS, 0.1 M, pH 7.4) containing KH_2PO_4 (0.1 M), Na_2HPO_4 (0.1 M) and KCl (0.1 M) was used as the electrolyte solution. $[Fe(CN)_6]^{4-/3-}$ (5 mM) containing KCl (0.1 M) was employed as a redox probe for cyclic voltammetry (CV) and electrochemical impedance spectroscopy (EIS) measurements. HAc-NaAc (0.1 M, pH 5.5) was used as working buffer solution. DNA hybridization buffer (HB, pH 7.4) containing NaCl (1.0 M), EDTA (1.0 mM) and Tris-HCl (10 mM) was used for preparing DNA solutions. Probe immobilization buffer (IB, pH 7.4) contained TCEP (10 mM), EDTA (1.0 mM), Tris-HCl (10 mM) and NaCl (0.1 M). 10 × TBE buffer was prepared by using Tris-HCl (890 mM), boric acid (890 mM) and EDTA (20 mM, pH 8.0) for gel electrophoresis experiments.

Exonuclease I (Exo I) and all of the oligonucleotides were synthesized and purified

by Sangon Biological Engineering Technology and Services Co., Ltd. (Shanghai, China). The sequences were listed in Table 1. Each oligonucleotide was pretreated with a procedure of heat incubation at 95 °C for 3 min and then cooled down to room temperature naturally. The obtained DNA solutions were stored at 4 °C for further use.

Table S1. Sequences of the oligonucleotides used in this experiment.

Name	Sequences (from 5' to 3')
OTA aptamer	Bio-GATCGGGTGTGGGTGGCGTAAAGGGAGCATCGGACA
OTA aptamer complementary DNA (cDNA)	TGTCCGATGCTCCCTTTACGCCACCCACACCCGATCGGGG TTTTATCGCAAAACCCC
Capture probe (SH-CP)	SH-GATCGGGTGTGGGTGGCGTAAAGGCGCCACCCACA
Assistant probe (AP)	CACCCGACTTATGTGGGTGGCGGAGCATCGGACACCCAC ACCCGA
Hairpin probe 1 (HP1)	CACCCGACTTATCGGGTGTGGG
Hairpin probe 2 (HP2)	TAAGTCGGGTGCCCACACCCGA

Apparatus

CV and SWV measurements were carried out with a CHI 660E electrochemical workstation (Shanghai Chen Hua Instrument, China). A PARSTAT 4000 electrochemical workstation (Princeton Applied Research, America) was used to realize EIS measurements. A three-electrode system is consisted of a saturated calomel electrode as reference electrode, a platinum wire as auxiliary electrode and the modified gold electrode (AuE) as working electrode. The morphologies and

structural analysis of different materials were measured by scanning electron microscope (SEM, Carl Zeiss ZEISS SIGMA), X-ray photoelectron spectroscopy (XPS, Perkin-Elmer) and powder X-ray diffraction (PXRD, Bruker D8).

Synthesis of Fe-MOF, Co-MOF and NH_2-Co-MOF

Fe-MOF was prepared by solvothermal method according to the literature [1] with some modification. Firstly, $FeCl_3 \cdot 6H_2O$ (162 mg) and BDC (49.8 mg) were dissolved in DMF (7.5 mL) and mixed well under ultrasonication for 10 min. After that, the mixture was sealed in an autoclave with a tetrafluoroethylene liner and kept heating at 105 °C for 20 h. After cooling to room temperature, the product (Fe-MOF) was collected by centrifugation and washing for several times with DMF and ethanol successively, and finally dried overnight at 70 °C. Co-MOF was synthesized by a similar method of Fe-MOF, except that 162 mg of $FeCl_3 \cdot 6H_2O$ was replaced by 142.8 mg of $CoCl_2 \cdot 6H_2O$ in the present work.

The synthesis of NH_2-Co-MOF was performed in the following manner. Typically, NH_2-BDC (54.3 mg) was dissolved in DMF (7.5 mL), and TEA (85 μL) was then dropped into the above solution and kept agitating vigorously for 10 min. Subsequently, $CoCl_2 \cdot 6H_2O$ (142.8 mg) was added into the above mixed solution, and it was heated to 105 °C for 20 h. After cooling to room temperature, the product of NH_2-Co-MOF was collected by centrifuged, washed, and then dried overnight at 70 °C.

Immobilization of biotin modified double-stranded DNA onto streptavidin magnetic beads (dsDNA-SAMB)

Briefly, biotin modified OTA aptamer (10 μL, 100 μM) and cDNA solution (10 μL, 100 μM) were added into 30 μL of DNA hybridization buffer and shocked evenly. Next, the mixture was annealed at 95 °C for 3 min and cooled to room temperature naturally to make the DNA strands hybridize adequately. Then, 50 μL of SAMB (1 mg mL^{-1}) was added to the above solution and kept reacting on a shaker for 60 min. Finally, the dsDNA-SAMB was collected by the magnetic separation and dispersed in 100 μL of DNA hybridization buffer, and stored at 4 °C for further use.

Exo I-assisted target recycling amplification

Firstly, 1 μL of OTA with a series of concentrations and 0.5 μL (10 U) of Exo I were simultaneously added into 10 μL of the prepared dsDNA-SAMB solution containing 1 μL of 10 × Exo I buffer and mixed uniformly by shocking. Subsequently, the solution was incubated at 37 °C for 90 min to accomplish the Exo I -assisted target recycling reaction. After that the cDNA in the supernatant solution was collected by the magnetic separation and stored at 4 °C.

Polyacrylamide gel electrophoresis (PAGE)

Six different kinds of DNA structures were analyzed with the freshly prepared polyacrylamide gel (16%) electrophoresis. The gel was carried in 10 × TBE buffer at 220 V for 60 min, and stained with GoldView solution for 25 min. The image of the gel was obtained using the Tanon Gel Imaging Systems.

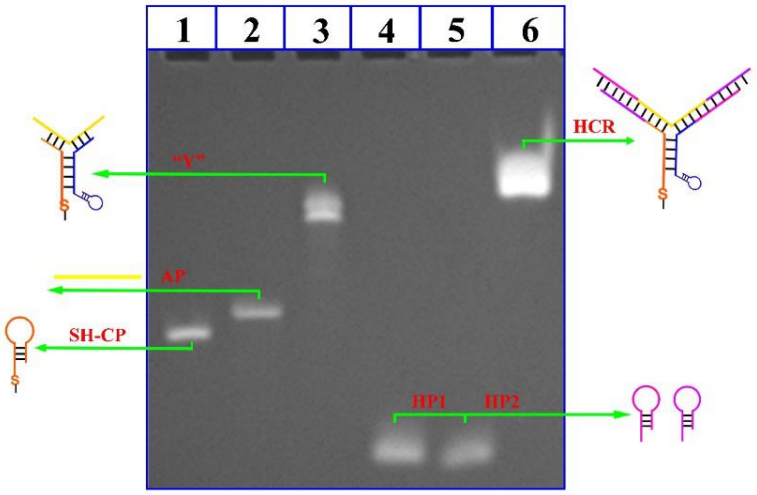

Fig. S1 Polyacrylamide gel (16%) electrophoresis analysis of different samples. Lane 1: SH-CP (10 μM); lane 2: AP (10 μM); lane 3: a mixture of SH-CP (10 μM), cDNA (10 μM) and AP (10 μM); lane 4: HP1 (10 μM); lane 5: HP2 (10 μM); lane 6: a mixture of SH-CP (10 μM), cDNA (10 μM), AP (10 μM), HP1 (100 μM) and HP2 (100 μM). Each solution was annealed at 90 °C for 5 min and then cooled to room temperature naturally.

Fabrication of electrochemical aptasensor

To obtain a mirror-like surface, the AuE was polished with 0.3 and 0.05 μm alumina powder successively and sonicated with ultrapure water. Initially, 15 μL of the prepared NH_2-Co-MOF solution was dropped onto the AuE *via* strong amino-Au affinity. Subsequently, the NH_2-Co-MOF/AuE was submerged into 20 μL of AuNs solution for 6 h at room temperature to obtain a large conductive surface area. Then the AuNs/NH_2-Co-MOF/AuE was further immersed into SH-CP solution (1.0 μM, IB) and incubated overnight at 4 °C for highly efficient immobilization of SH-CP with the formation of Au-S link between the AuNs layer and the -SH of CP. Lastly, 15 μL of HT (1%) was dropped onto the electrode surface for 1 h to block the nonspecific binding sites. After every step, the modified electrode was cleaned with ultrapure

water gently to remove the physical adsorption. Finally, the resulting aptasensor was stored at 4 °C for the further use.

Measurement Procedure

Before measurements, the mixture of the collected cDNA (produced from the target recycling reaction and obtained by the magnetic separation) and 1 μL of AP (10 μM) was incubated on the HT/SH-CP/AuNs/NH_2-Co-MOF/AuE for 2 h at 37 °C to form the DNA Y-junction structure on the sensing surface. After cleaning with ultrapure water, 10 μL of homogeneous solution consisting of Thi (8 μL, 1 mg mL^{-1}), HP1 (8 μL, 100 μM) and HP2 (8 μL, 100 μM) was dropped onto the resultant aptasensor and incubated at 37 °C for 1 h to accomplish the hybridization chain reaction, meanwhile, numerous of redox molecule (Thi) was embedded into the dsDNA grooves *via* electrostatic adsorption. After rinsing with ultrapure water to remove nonspecific adsorption, the prepared aptasensor was measured in HAc-NaAc solution (0.1 M, pH 5.5) to examine SWV response.

SWV characterization was taken in HAc-NaAc solution (0.1 M, pH 5.5) and the potential range was from 0.1 V to -0.5 V. The process of the electrode fabrication was characterized by CV and EIS measurements in PBS (0.1 M, pH 7.4) containing 5 mM $[Fe(CN)_6]^{4-/3-}$ as redox probe. CV measurements were performed at a scan rate of 0.1 V s^{-1} from -0.2 V to 0.6 V. EIS measurements were carried out with the alternative voltage of 5 mV and the frequency range was from 0.01 Hz to 100 KHz.

Results and discussion

Synthesis and characterization of the as-synthesized NH_2-Fe-MOF

NH_2-Fe-MOF was prepared through solvothermal reaction. The morphology and structure of the as-synthesized NH_2-Fe-MOF were characterized by SEM and PXRD, respectively. As shown in Fig. S2A, there are two different morphologies (octahedron and spindle-like). At the same time, PXRD pattern in Fig. S2B proves that the resulting NH_2-Fe-MOF is not a homogeneous, it may be composed of MIL-101(Fe) and MIL-88(Fe). The electrocatalytic activity for redox molecule (Thi) can be seen in Fig. S2D, compared with Fe-MOF (Fig. S2C) and NH_2-Co-MOF (Fig. S2E), the electrocatalytic activities of the MOFs followed the order NH_2-Co-MOF > NH_2-Fe-MOF > Fe-MOF.

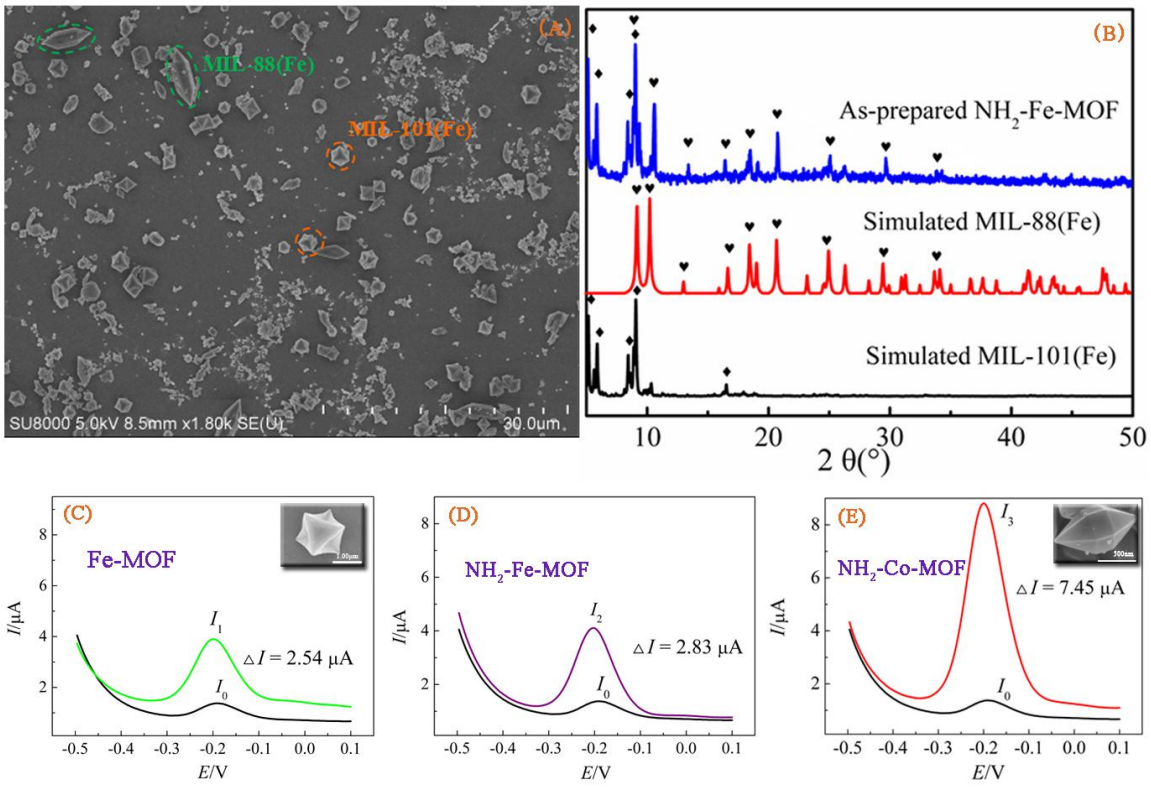

Fig. S2 (A) SEM image and (B) PXRD pattern of NH_2-Fe-MOF, and SWV responses of three synthesized MOFs (insert: SEM images): Fe-MOF (C), NH_2-Fe-MOF (D) and NH_2-Co-MOF (E) modified AuE in 0.1 M HAc-NaAc solution (pH 5.5) containing 35 μM Thi.

XPS characterization of NH_2-Co-MOF

XPS was employed to investigate the oxidation states of cobalt in the NH_2-Co-MOF. As displayed in Fig. S3, in the full survey spectra (Fig. S3, left) of the as-synthesized NH_2-Co-MOF, the main peaks can be clearly indexed to Co 2p, N 1s, O 1s, and C 1s regions. In Co 2p spectrum (Fig. S3, right), the Co 2p peak is divided into two sets of satellite peaks (785.11 eV, 801.05 eV) and spin-orbit doublets (Co $2p_{1/2}$ and Co $2p_{3/2}$) [2-3]. The presence of satellite peaks has been reported to support in the presence of Co(II) species [4-5], and the peak separation between the two parental peaks at 780.9 and 796.1 eV is corresponding to Co(III) species [6]. Based on the observations above, it is reasonable to believe that Co^{2+}/Co^{3+} species are co-existed in the as-synthesized NH_2-Co-MOF.

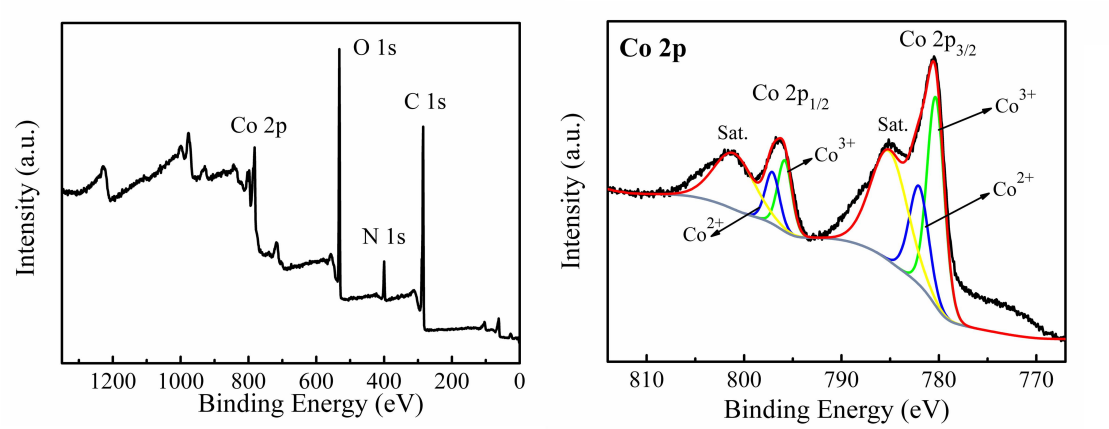

Fig. S3. XPS spectra of the as-synthesized NH_2-Co-MOF: full spectra (left) and high-resolution Co 2p spectrum (right).

Comparison of different electrocatalysis ability of NH_2-Co-MOF and HRP/H_2O_2 system for Thi

The comparison experiment of NH_2-Co-MOF and HRP/H_2O_2 system for the electrocatalysis of Thi was investigated under the same conditions. As shown in Fig

S4, the black line shows the CV response of Thi, while the red line and blue line represents the NH_2-Co-MOF (A) and HRP/H_2O_2 system (B), respectively. It can be noted that the cathodic peak current significantly increased, and the peak potential shifted by −34~−27 mV. Moreover, SWV results (C and D) are in good accordance with CVs. As supported by the above results, the obtained NH_2-Co-MOF could efficiently catalyze the electrochemical reduction of thionine into leucothionine, similar to the well-studied HRP/H_2O_2 system [7].

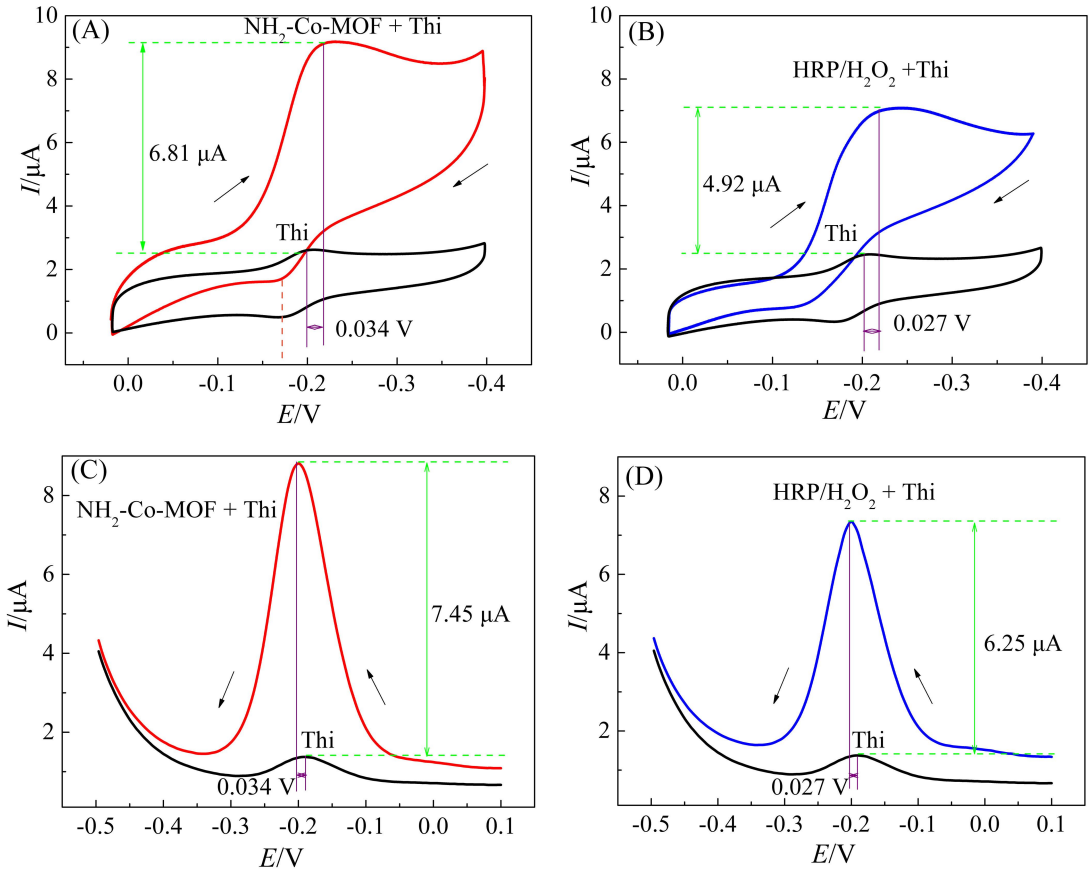

Fig. S4 The comparison experiment of NH_2-Co-MOF (A, C) and HRP/H_2O_2 system (B, D) for the electrocatalysis of Thi. CV (A, B) and SWV (C, D) signals were measured in 0.1 M HAc-NaAc buffer (pH 5.5) ontaining 35 μM Thi.

Optimization of experimental conditions

In order to achieve the best sensing performance and maximize the sensitivity and efficiency, several experimental parameters including the concentration and the incubation time of Exo I, the concentration of SH-CP and the incubation time of hybridization reaction are optimized. As shown in Fig. S5A, with the concentration of SH-CP increasing from 0.1 to 1.9 μM, SWV response increases gradually, and the maximum peak current occurs at 1.0 μM. Fig. S5B reveals the effect of the concentration of Exo I in the target recycling amplification from 1 to 20 U. The current responses increased with increasing concentration of Exo I until the concentration reached 10 U. The influence of the incubation time of Exo I is shown in Fig. S5C. It can be noted that the current responses increase with the incubation time rapidly up to 90 min, then there was a slightly decrease with the incubation time further increased. Therefore, 90 min was the most appropriate incubation time. Moreover, the effect of incubation time of hybridization reaction is also investigated (Fig. S5D). With the hybridization time increasing from 20 to 90 min, the SWV responses increased significantly and reached a maximum value at 60 min. As a result, 60 min was adopted as the optimal hybridization time for the subsequent study.

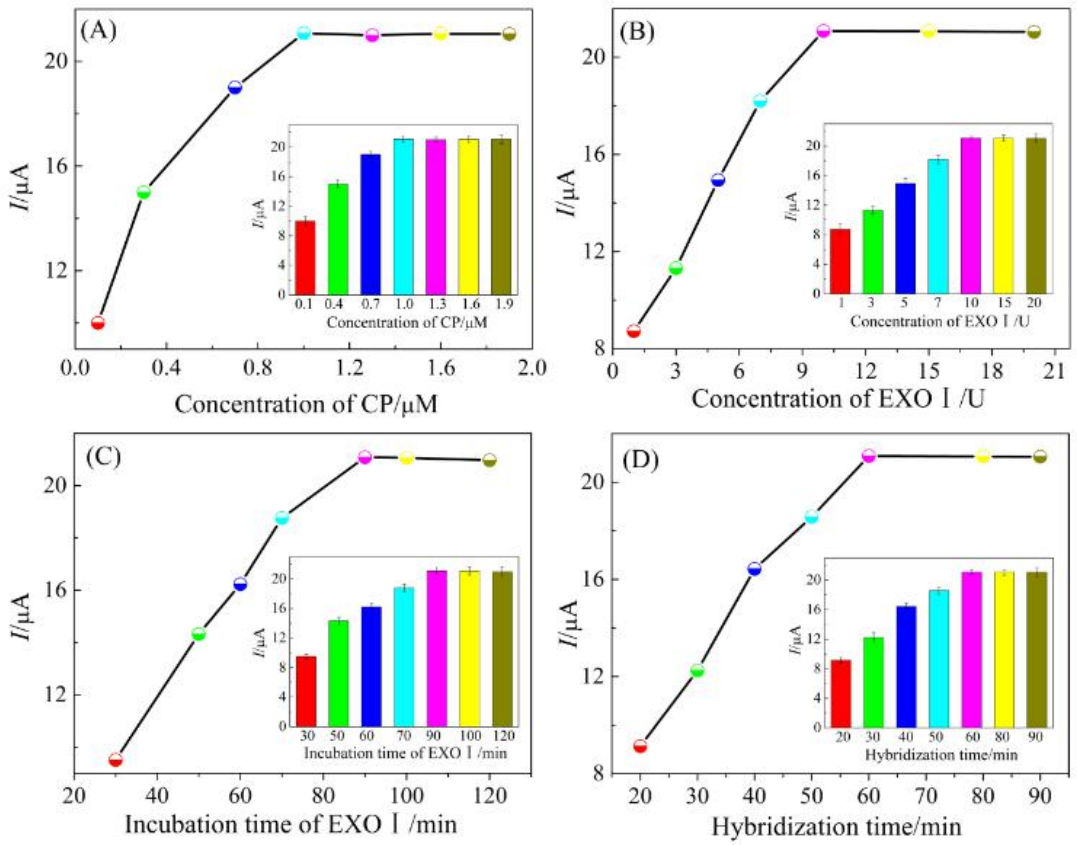

Fig. S5 Optimization of experimental conditions by the proposed aptasensor incubated with OTA (0.1 ng mL^{-1}) and measured in HAc-NaAc buffer solution (pH 5.5): (A) influence of the concentration of SH-CP on the AuE; (B) effect of the concentration of Exo I in the target recycling reaction; (C) affect of the incubation time of Exo I in the target recycling reaction; (D) impact of hybridization chain reaction time.

Comparison of different signal amplification strategies

In order to verify the signal amplification capability of the designed aptasensor, three different amplification strategies are compared to detect OTA (0.1 ng mL^{-1}) under the same conditions, and the results are displayed in Fig. S6. After incubation with cDNA (produced from the target recycling amplification without Exo I) on the modified HT/SH-CP/AuNs/AuE, there is a weak SWV response (curve a, I_a = 6.58 μA) corresponding to the reversible redox molecule of Thi. It is worth noting that

when Exo I was added to the target recycling reaction solution, a significantly enhanced SWV signal is obtained (curve b, I_b = 10.04 μA). The current value increased about 1.5 times than the initial current signal (curve a, I_a), which was attributed to the increasing amount of cDNA (produced from the target recycling reaction and obtained by the magnetic separation), and further hybridize with SH-CP and AP to form a ternary "Y" junction structure on the electrode surface. Subsequently, numerous of redox molecule (Thi) was embedded into the "Y" grooves *via* electrostatic adsorption during the hybridization chain reaction, thus, giving a sensitive SWV response. In order to evaluate the signal amplification ability of as-synthesized NH_2-Co-MOF, HT/SH-CP/AuNs/NH_2-Co-MOF/AuE without Exo I-assisted target recycling amplification was investigated. As seen from curve c, an obvious enhanced SWV signal is observed (I_c = 12.09 μA), which clearly demonstrate that NH_2-Co-MOF could effectively electrocatalyze Thi to amplify electrochemical signal even in the absence of H_2O_2. Surprisingly, when NH_2-Co-MOF and Exo I was employed for signal amplification at the same time, the highest signal is noticed (curve d, I_d = 21.08 μA), the current value is about 3.2 times than the initial current signal. The above results clearly illustrate that the excellent sensitivity of the aptasensor can be ascribed to the Exo I-assisted target recycling reaction and the excellent catalytic amplification of NH_2-Co-MOF.

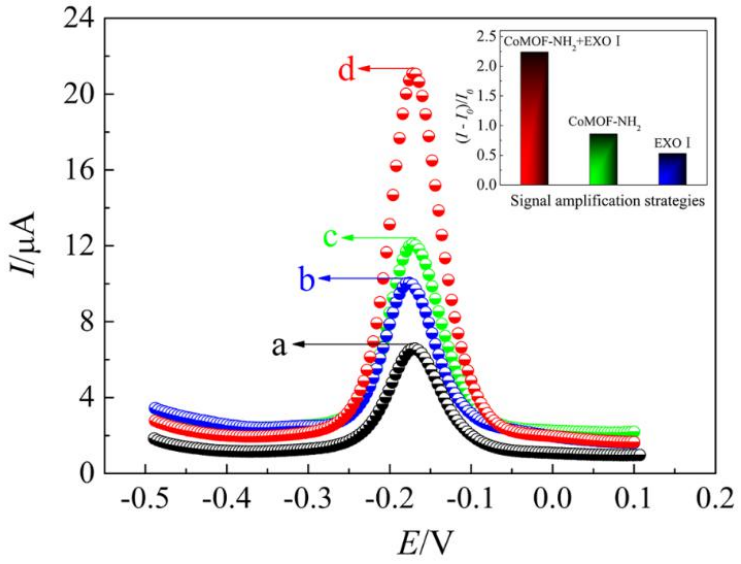

Fig. S6 SWV responses of different signal amplification strategies for incubation with cDNA on the modified HT/SH-CP/AuNs/AuE for the detection of OTA (0.1 ng mL^{-1}) in HAc-NaAc buffer solution (pH 5.5): (a) without signal amplification; (b) with Exo I-assisted signal amplification strategy; (c) with NH_2-Co-MOF assisted no substrate nanoelectrocatalysis; (d) with NH_2-Co-MOF and Exo I-assisted signal amplification strategy (Insert: The ratio of $(I - I_0)/I_0$, I is the different SWV value with different signal amplification strategies, I_0 was the initial current signal).

Table S2. Comparison of our research with other published methods for OTA detection.

Detection techniques	Linear ranges/ng mL^{-1}	Detection limits	Ref
Colorimetric assay	0.5-100	30 pg mL^{-1}	[8]
Enzyme-linked immunosorbent assay	0.125-8	103.2 pg mL^{-1}	[9]
Fluorescence	0.05-20	13 pg mL^{-1}	[10]
Fluorescence	1-30	0.5 ng mL^{-1}	[11]
Differential pulse voltammetry	0.01-50	5.6 pg mL^{-1}	[12]
Differential pulse voltammetry	0.15-5	0.07 ng mL^{-1}	[13]
Surface plasmon resonance	0.2-40	0.005 ng mL^{-1}	[14]
Square wave voltammetry	0.000001-1	0.3 fg mL^{-1}	This work

Table S3. Comparison of the as-synthesized NH_2-Co-MOF with other nanomaterials for signal amplification.

Catalytic materials	Substrates	Detecting techniques	Targets	Linear ranges	Detection limits	Ref
Fe-MOF (MIL-68)	H_2O_2	Colorimetric assay	Ascorbic acid	30-485 μM	6 μM	[15]
Fe-MOF	H_2O_2	Differential pulse voltammetry	Lead(II)	0.03-1000 nmol L^{-1}	0.02 nmol L^{-1}	[16]
Ce-MOF	H_2O_2	Differential pulse voltammetry	Lipopolysaccharide	10 fg mL^{-1}- 100 ng mL^{-1}	3.3 fg mL^{-1}	[17]
Ce-MOF	H_2O_2	Colorimetric assay	Glutathione	0-40 μM	0.129 μM	[18]
MnTMPyP	H_2O_2	Electrochemical impedance spectroscopy	Nuclear factor kappa B	0.01-20 nM	7 pM	[19]
NiPd hollow nanoparticles	H_2O_2	Colorimetric assay	Glucose	0.005-0.5 mM	4.2 μM	[20]
NH_2-Co-MOF	-	Square wave voltammetry	Ochratoxin A	1 fg mL^{-1}-1 ng mL^{-1}	0.33 fg mL^{-1}	This work

Real sample analysis

We further validated the practical application ability of the proposed assay for OTA determination in red wine with the standard addition method. As shown in Table. S4, the recoveries of OTA in the red wine samples were in the range of 90.0-105.0% and *RSD* in the range of 3.4-6.8%. This evaluation of the proposed aptasensor illuminated that it has the potential for the detection of OTA in real wine samples.

Table S4. Detection of OTA added in red wine (n = 3) with the proposed method.

Samples	Spiking value (ng mL^{-1})	Assayed value (ng mL^{-1})	Recovery/%	*RSD*/%
1	0.01	0.009	90.0	5.2
2	0.10	0.105	105.0	3.4
3	0.50	0.47	94.0	6.8
4	10.0	10.1	101.0	4.1

References

[1] K. L. T. Taylor-Pashow, J. D. Rocca, Z. G. Xie, S. Tran and W. B. Lin, *J. Am. Chem. Soc*., 2009, **131**, 14261.

[2] R. M. Li, R. Che, Q. Liu, S. Z. Su, Z. S. Li, H. S. Zhang, J. Y. Liu, L. H. Liu and J. Wang, *Journal of Hazardous Materials*, 2017, **338**, 167.

[3] J. Huang, W. X. Qian, H. F. Ma, H. T. Zhang and W. Y. Ying, *RSC Adv.*, 2017, **7**, 33441.

[4] D. C. Hong, J. Jung, J. Park, Y. Yamada, T. Suenobu, Y. M. Lee, W. Nam and S. Fukuzumi, *Energy & Environmental Science*, 2012, **5**, 7606.

[5] F. Y. Song, Y. Ding, B. C. Ma, C. M. Wang, Q. Wang, X. Q. Du, S. Fu and J. Song, *Energy & Environmental Science*, 2013, **6**, 1170.

[6] Y. Gartia, C. M. Felton, F. Watanabe, P. K. Szwedo, A. S. Biris, N. Peddi, Z. A. Nima and A. Ghosh, *ACS Sustainable Chemistry & Engineering*, 2014, **3**, 97.

[7] T. T. Zheng, Q. F. Zhang, S. Feng, J. J. Zhu, Q. Wang and H. Wang, *J. Am. Chem. Soc*., 2014, **136**, 2288.

[8] C. Q. Wang, J. Qian , K. Wang, X. W. Yang, Q. Liu, N. Hao, C. K. Wang, X. Y. Dong and X. Y. Huang, *Biosens. Bioelectron*., 2016, **77**, 1183.

[9] Y. Wang, X. F. Hu, Y. F. Pei, Y. N. Sun, F. Y. Wang, C. M. Song, M. Q. Yin, R. G. Deng, Z. X. Li and G. P. Zhang, *Anal. Methods*, 2015, **7**, 1849.

[10] S. Wang, Y. J. Zhang, G. S. Pang, Y. W. Zhang and S. J. Guo, *Anal. Chem*., 2017, **89**, 1704.

[11] X. F. Chu, X. W. Dou, R. Z. Liang, M. H. Li, W. J. Kong, X. H. Yang, J. Y. Luo, M. H. Yang and M. Zhao, *Nanoscale*, 2016, **8**, 4127.

[12] A. L. Sun, Y. F. Zhang, G. P. Sun, X. N. Wang and D. P. Tang, *Biosens. Bioelectron*., 2017, **89**, 659.

[13] R. K. Mishra, A. Hayat, G. Catanante, G. Istamboulie and J. L. Marty, *Food Chemistry*, 2016, **19**2, 799.

[14] M. Bianco, A. Sonato, A. De Girolamo, M. Pascale, F. Romanato, R. Rinaldi and V. Arima, *Sensors and Actuators B*, 2017, **241**, 314.

[15] J. W. Zhang, H. T. Zhang, Z. Y. Du, X. Q. Wang, S. H. Yu and H. L. Jiang, *Chem. Commun*., 2014, **50**, 1092.

[16] X. Wang, C. L. Yang, S. J. Zhu, M. Yan, S. G. Ge and J. h. Yu, *Biosens. Bioelectron*., 2017, **87**, 108.

[17] W. J. Shen, Y. Zhuo, Y. Q. Chai and Ruo Yuan, *Biosens. Bioelectron*., 2016, **83**, 287.

[18] Y. H. Xiong, S. H. Chen, F. G. Ye, L. J. Su, C. Zhang, S. F. Shen and S. L. Zhao, *Chem. Commun*., 2015, **51**, 4635

[19] K. F. Peng, H. W. Zhao, P. Xie, S. Hu, Y. L. Yuan, R. Yuan and X. F. Wu, *Biosens. Bioelectron*., 2016, **81**, 1.

[20] Q. Q. Wang, L. L. Zhang, C. S. Shang, Z. Q. Zhang and S. J. Dong, *Chem. Commun*., 2016, **52**, 5410.